Increased Tumor Necrosis Factor α–Converting Enzyme Activity Induces Insulin Resistance and Hepatosteatosis in Mice

Loredana Fiorentino,[1]* Alessia Vivanti,[1]* Michele Cavalera,[1] Valeria Marzano,[1,2] Maurizio Ronci,[1,2] Marta Fabrizi,[1] Stefano Menini,[3] Giuseppe Pugliese,[3] Rossella Menghini,[1] Rama Khokha,[4] Renato Lauro,[1] Andrea Urbani,[1,2] and Massimo Federici[1]

Tumor necrosis factor α–converting enzyme (TACE, also known as ADAM17) was recently involved in the pathogenesis of insulin resistance. We observed that TACE activity was significantly higher in livers of mice fed a high-fat diet (HFD) for 1 month, and this activity was increased in liver > white adipose tissue > muscle after 5 months compared with chow control. In mouse hepatocytes, C_2C_{12} myocytes, and 3T3F442A adipocytes, TACE activity was triggered by palmitic acid, lipolysaccharide, high glucose, and high insulin. TACE overexpression significantly impaired insulin-dependent phosphorylation of AKT, GSK3, and FoxO1 in mouse hepatocytes. To test the role of TACE activation *in vivo*, we used tissue inhibitor of metalloproteinase 3 (Timp3) null mice, because Timp3 is the specific inhibitor of TACE and *Timp3*$^{-/-}$ mice have higher TACE activity compared with wild-type (WT) mice. *Timp3*$^{-/-}$ mice fed a HFD for 5 months are glucose-intolerant and insulin-resistant; they showed macrovesicular steatosis and ballooning degeneration compared with WT mice, which presented only microvesicular steatosis. Shotgun proteomics analysis revealed that *Timp3*$^{-/-}$ liver showed a significant differential expression of 38 proteins, including lower levels of adenosine kinase, methionine adenosysltransferase I/III, and glycine *N*-methyltransferase and higher levels of liver fatty acid-binding protein 1. These changes in protein levels were also observed in hepatocytes infected with adenovirus encoding TACE. All these proteins play a role in fatty acid uptake, triglyceride synthesis, and methionine metabolism, providing a molecular explanation for the increased hepatosteatosis observed in *Timp3*$^{-/-}$ compared with WT mice. *Conclusion:* We have identified novel mechanisms, governed by the TACE–Timp3 interaction, involved in the determination of insulin resistance and liver steatosis during overfeeding in mice. (HEPATOLOGY **2009;50:000-000.**)

Pandemic obesity is now considered the underlying basis for the increasing prevalence of chronic metabolic-inflammatory diseases including type 2 diabetes, nonalcoholic fatty liver disease (NAFLD) and atherosclerosis.[1] Although NAFLD is an emerging metabolic complication of obesity, its pathogenic mechanisms are still unclear.[1]

The contribution of insulin resistance to the development of fatty liver occurs in part by deficient control of lipid storage in white adipose tissue and in part by altered

Abbreviations: ADK, adenosine kinase; BSA, bovine serum albumin; FABP1, fatty acid–binding protein 1; GFP, green fluorescent protein; GNMT, glycine N-methyltransferase; HFD, high-fat diet; JNK, c-Jun N-terminal kinase; MAT1A, methionine adenosysltransferase 1A; MATI/III, methionine adenosysltransferase I/III; mRNA, messenger RNA; NAFLD, nonalcoholic fatty liver disease; PA, palmitic acid; SV40, PCR, polymerase chain reaction; Simian virus 40; SD, standard deviation; TACE, tumor necrosis factor α–converting enzyme; Timp3, tissue inhibitor of metalloproteinase 3; TNF-α, tumor necrosis factor α; WAT, white adipose tissue; WT, wild-type.

From the [1]Department of Internal Medicine, University of Rome Tor Vergata, Rome, Italy; [2]S. Lucia Research Institute, Rome, Italy; the [3]Department of Clinical Sciences, Sapienza University of Rome, Rome, Italy; and the [4]Ontario Cancer Institute, University of Toronto, Toronto, Ontario, Canada.

Received April 1, 2009; accepted August 12, 2009.

Supported in part by grants from Telethon (GGP-08065), Juvenile Diabetes Research Foundation (Research Grant 1-2007-665), Società Italiana di Diabetologia (Italian Society of Diabetology) (Research Grant 2007), the Italian Ministry of University (PRIN 2006/2008), Ministry of Health Research Grants (all to M. F.), and Fondazione Roma (to M. F. and A. U.).

**These authors contributed equally to this work.*

Address reprint requests to: Massimo Federici, M.D., Department of Internal Medicine, University of Rome Tor Vergata, Via Montpellier 1, 00133 Rome, Italy. E-mail: federicm@uniroma2.it; fax: (39)-0672596890.

Published online in Wiley InterScience (www.interscience.wiley.com).

DOI 10.1002/hep.23250

Potential conflict of interest: Nothing to report.

Additional Supporting Information may be found in the online version of this article.

control of hepatic lipogenesis and mitochondrial fatty acid oxidation.[2] Increased release of inflammatory factors or diminished secretion of protective adipokines from dysfunctional adipose tissue can predispose hepatocytes to accumulate lipids in obese individuals.[3] Further evolution to fibrosis and steatohepatitis may involve activation of hepatic stellate cells and Kupffer cells by insulin resistance–related factors.[4] Tumor necrosis factor α (TNF-α) is among the cytokines involved in linking nutrient availability to innate immune activation and development of fatty liver disease.[5] Local/paracrine regulation of TNF-α release from plasma membrane through its ectodomain shedding is regulated by TACE.[6] TACE is naturally inhibited by tissue inhibitor of metalloproteinase 3 (Timp3), which has the potential to regulate other ADAM and matrix metalloproteinases during immune responses.[6] Activation of TACE is triggered by way of protein kinase C and extracellular signal-regulated kinase signals upon several stimuli, including metabolic ones such as hyperinsulinemia.[7-9] We have recently shown that whereas lack of Timp3 alone has no gross effect on insulin resistance and glucose tolerance in mice fed a regular diet, its deficiency accelerates liver inflammation and steatosis only if coupled to genetic-dependent and nutrient-dependent insulin resistance.[10-12] The TACE/Timp3 system is therefore emerging as a pivotal mediator between metabolic stimuli and innate immunity, although the temporal and spatial regulation of this activation remains unknown. We coupled murine and cellular models to proteomic technologies to show that hepatic TACE overactivity is central to the development of fatty liver disease.

Materials and Methods

Reagents. Free fatty acid–free, low endotoxin bovine serum albumin (BSA), palmitic acid, lipolysaccharide, insulin, glucose, c-Jun N-terminal kinase (JNK) inhibitor SP600125, and other common chemicals were obtained from Sigma Aldrich (St. Louis, MO). A list of antibodies is available in the Supporting Information.

Cell Culture. 3T3-F442A preadipocytes, C_2C_{12} myocytes, and Simian virus 40 (SV40)-tranformed hepatocytes were grown and differentiated as described.[13-15]

Metabolic Treatments. Palmitic acid was dissolved in methanol by heating at 75°C and mixing, then loaded onto free fatty acid–free low endotoxin BSA by way of sonication and gently shaking overnight at 37°C to yield a 5-mM solution of palmitic acid in 5% BSA. Before treatments, all cells were serum-starved in 0.5% BSA overnight and then treated for 2 hours with 0.5 mM palmitic acid (PA) alone or in combination with the JNK inhibitor SP600125 (20 μM). For glucose treatment, cells were either grown in low-glucose medium (C_2C_{12} and hepatocytes) or were glucose-starved for 4 hours before treatment (3T3-F442A).

TACE Activity. TACE activity was determined using the SensoLyte 520 TACE Activity Assay Kit (AnaSpec, San Jose, CA) according to the manufacturer's protocol. Thirty micrograms tissue proteins or 20 μg cell proteins were used for the assay. A reaction was started by adding 40 μM of the fluorophoric QXL520/5FAM FRET substrate. Fluorescence of the cleavage product was measured in a fluorescence microplate reader (FLx800, BIO-TEK Instruments, Winooski, VT) at lex 490 nm and lem 520 nm.

Adenovirus Infection. Adenoviruses expressing green fluorescent protein (GFP) only or GFP and TACE (Vector Biolabs, Philadelphia, PA) were used to infect SV40-tranformed hepatocytes. The infection was carried out at 500 pfu/cells in α minimum essential medium supplemented with 0.2% BSA for 6 hours at 33°C. The virus-containing medium was then removed, and cells were incubated for 24 hours in α minimum essential medium supplemented with 4% fetal bovine serum before being differentiated and treated as described.

Animal Models and Analytical Procedures. *Timp3*$^{-/-}$ mice on a C57/BL6 background have been described,[16] as have metabolic testing procedures[10-12] (see also Supporting Information). Animal studies were approved by the University of Tor Vergata Animal Care and Use Committee. All animals received human care according to the criteria outlined in the "Guide for the Care and Use of Laboratory Animals" prepared by the National Academy of Sciences and published by the National Institutes of Health (NIH publication 86-23, revised 1985).

Extraction of Timp3 for Western Blots. For the extraction of matrix-bound Timp3, tissues were treated as described.[10]

Histology and Quantification of Liver Lesions. Histology was perfomed as described.[12] (See Supporting Information for details.)

Gene Expression Analysis. Total RNA was isolated from wild-type (WT) and *Timp3*$^{-/-}$ mice and from SV40-transformed hepatocytes using Trizol reagent (Invitrogen Corp, Carlsbad, CA). Two micrograms of total RNA were reverse-transcribed into complementary DNA using the High Capacity cDNA Archive kit (Applied Biosystems, Foster City, CA). Quantitative real-time polymerase chain reaction was performed using an ABI PRISM 7700 System and TaqMan reagents (Applied Biosystems). Each reaction was performed in triplicate using standard reaction conditions. The Applied Biosystems primers used are listed in the Supporting Methods.

Protein Identification and Quantization by LC-MS^E and Ingenuity Pathway Analysis. Shotgun proteomics and ingenuity pathways analysis were performed as described[17,18] and are reported in an extended version in the Supporting Information.

Liver Methionine Metabolism Assay. Assays for *S*-adenosylmethionine and *S*-adenosylhomocysteine in liver and cells—methionine and homocysteine in serum—were performed as described[19] and are reported in an extended version in the Supporting Methods.

Statistical Analysis. Results of the experimental studies are expressed as the mean ± standard deviation as indicated. Statistical analysis was performed using one-way analysis of variance, two-way analysis of variance, or an unpaired Student *t* test as appropriate. Values of $p < 0.05$ were considered statistically significant.

Results

TACE Activation Is Induced by Metabolic Stimuli In Vitro and Impairs Insulin Signaling. We have recently described that regulation of TNF-α release from plasma membrane through its ectodomain shedding by TACE has a role in accelerating liver inflammation and steatosis when coupled with an insulin-resistant environmental and genetic background.[10-12] Because TACE haploinsufficiency protects from lipotoxicity and glucotoxicity in an in vivo model, we analyzed three different *in vitro* cell culture models—3T3-F442A adipocytes, C_2C_{12} myocytes, and SV40-tranformed hepatocytes—to study mechanisms that link metabolic dysfunction to TACE activation. TACE activity was significantly increased by treatment with a free fatty acid, palmitic acid (0.5 mM; 2 hours), lipolysaccharide (200 ng/mL; 2 hours), high glucose (15 mM; 2 hours), or high insulin (10^{-7} M; 2 hours) (Fig. 1A). To test whether increased TACE activity is a downstream effector of metabolic toxicity to impaired insulin action, we overexpressed TACE by way of adenoviral vectors. This resulted in increased TACE activity (Fig. 1B). Inhibition of JNK activity by SP600125 partially reversed the effect of palmitic acid and TACE overexpression on TACE activity (Fig. 1C,D). In a preliminary set of results, we observed that TACE overexpression impairs ligand-dependent phosphorylation of the insulin receptor β subunit at different insulin concentrations (10^{-9}M and 10^{-7}M) and time points (Supporting Fig. 1). Next, we analyzed downstream elements of insulin signaling involved in the control of glucose and lipid metabolism. We found that phosphorylation of AKT on serine 473, FoxO1 on serine 256, and GSK3α/β on serine 9/21 were all consistently reduced by increased TACE activity (Fig. 1E).

TACE Expression and Activity Are Modulated During HFD. To identify tissues in which TACE activity may affect glucose and lipid metabolism, we analyzed its activation in white adipose tissue (WAT), muscle, and liver of C57/BL6 mice fed either a high-fat diet (HFD) or chow for 5, 10, and 20 weeks after weaning. We found that TACE activity was significantly increased by HFD first in liver at 10 weeks and continued to be increased after 20 weeks of HFD compared with chow (Fig. 2A). Both WAT and muscle also displayed increased TACE activity by this time point. Next, we analyzed the expression levels of TACE and its inhibitor Timp3 in all three tissues and found that whereas increased TACE activation associated with a mild increase of TACE expression in WAT and liver, a more significant decrease of Timp3 expression occurs at both messenger RNA (mRNA) and protein levels in all three tissues (Fig. 2B,C).

Overall, these results suggest that prolonged metabolic stress is associated with increased TACE activity and decreased Timp3 expression.

Impaired Glucose Tolerance and Steatohepatitis in Timp3$^{-/-}$ Mice Fed a HFD for 20 Weeks. Timp3$^{-/-}$ mice manifest increased TACE activity, especially in the liver.[16]

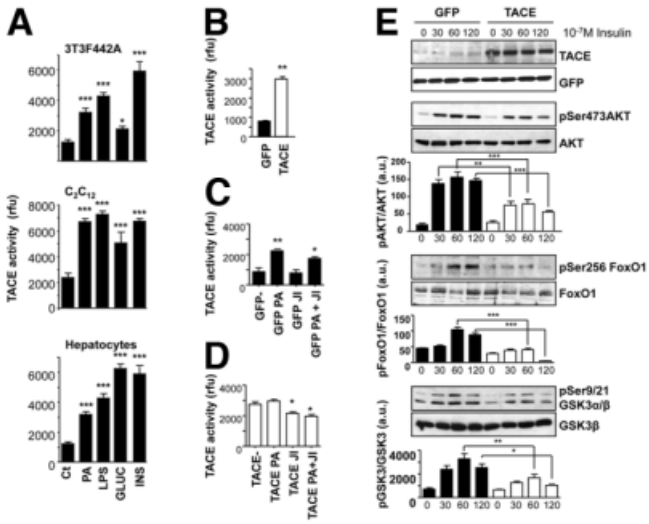

Fig. 1. TACE activity is induced by metabolic stimuli *in vitro* and impairs insulin signaling. (A) 3T3F442A adipocytes (top), C_2C_{12} myocytes (middle), and SV40-transformed hepatocytes (bottom) were treated with 0.5 mM palmitic acid, 200 ng/mL lipolysaccharide, 15 mM glucose or 10^{-7} M insulin for 2 hours and then analyzed for TACE activity. (B) SV40-transformed hepatocytes were infected with adeno-GFP or adeno-GFP-TACE and then analyzed for TACE activity. (C,D) SV40-transformed hepatocytes infected with adeno-GFP or adeno-GFP-TACE were treated with 0.5 mM PA in the presence or absence of 20 μM JNK inhibitor SP600125; data are expressed as the mean ± standard deviation (SD) (n = 3). $^{**}P < 0.01$ versus GFP, $^{*}P < 0.05$ versus GFP-PA (C). $^{*}P < 0.05$ versus both TACE and TACE PA (D). (E) SV40-transformed hepatocytes were infected with adeno-GFP or adeno-GFP-TACE and then stimulated with 10^{-7} M insulin for different time lengths. Cells were lysed and subjected to western blotting to detect TACE overexpression, and Ser473 AKT, Ser256 FoxO1, and Ser9/21 GSK3α-β phosphorylation, matched against total protein levels. Data are expressed as the mean ± SD (n = 3-5). $^{***}P < 0.001$. $^{**}P < 0.005$. $^{*}P < 0.05$.

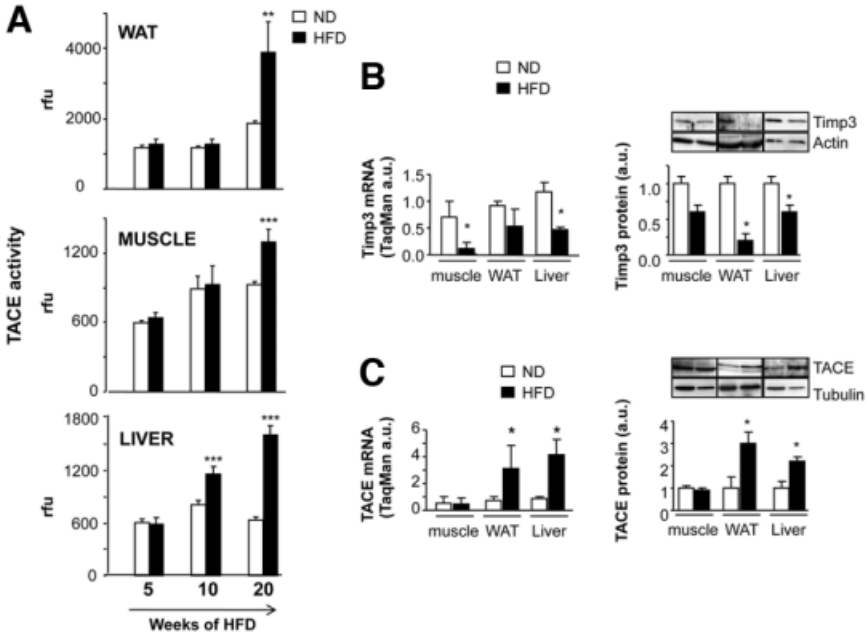

Fig. 2. TACE expression and activity are modulated during a HFD. C57/BL6 mice were fed either a HFD or chow diet for different periods. WAT, muscle, and livers were homogenated to analyze (A) TACE activity, (B) Timp3, and (C) TACE protein and mRNA levels were quantified by way of western blotting and real-time PCR, respectively, from muscle, WAT, and livers of HFD or chow-fed mice. Data are expressed as the mean ± SD (n = 3). ***$P < 0.001$. **$P < 0.005$. *$P < 0.05$.

However, we have previously shown that metabolic homeostasis in *Timp3*$^{-/-}$ mice is similar to that of WT littermates at 24 weeks of age, when both are fed chow, offering the ideal scenario to study the interaction between increased TACE activity and the prolonged metabolic stress caused by a diet rich in lipids. *Timp3*$^{-/-}$ mice fed a HFD for 20 weeks exhibited a weight similar to that of WT mice (Fig. 3A); however, *Timp3*$^{-/-}$ animals showed significantly increased fasting and fed glucose and insulin levels (Fig. 3B,C), increased aminotransferases (Fig. 3D), and worsened glucose tolerance (Fig. 3E) and insulin sensitivity (Fig. 3F) compared with WT littermates.

Analysis of liver function and histology revealed that after 20 weeks of HFD, *Timp3*$^{-/-}$ mice manifested increased TACE activity (Fig. 4A) and macrovesicular steatosis with features of ballooning degeneration as seen in grade 2 human steatohepatitis (Fig. 4C,E) compared with only microvesicular steatosis in WT livers (Fig. 4B,D). Analysis of the expression of several transcription factors known to regulate lipid and carbohydrate metabolism revealed that *Timp3*$^{-/-}$ livers had significantly higher levels of liver X receptor α and carbohydrate response element binding protein 1 along with significantly reduced levels of peroxisome proliferator-activated receptor δ and

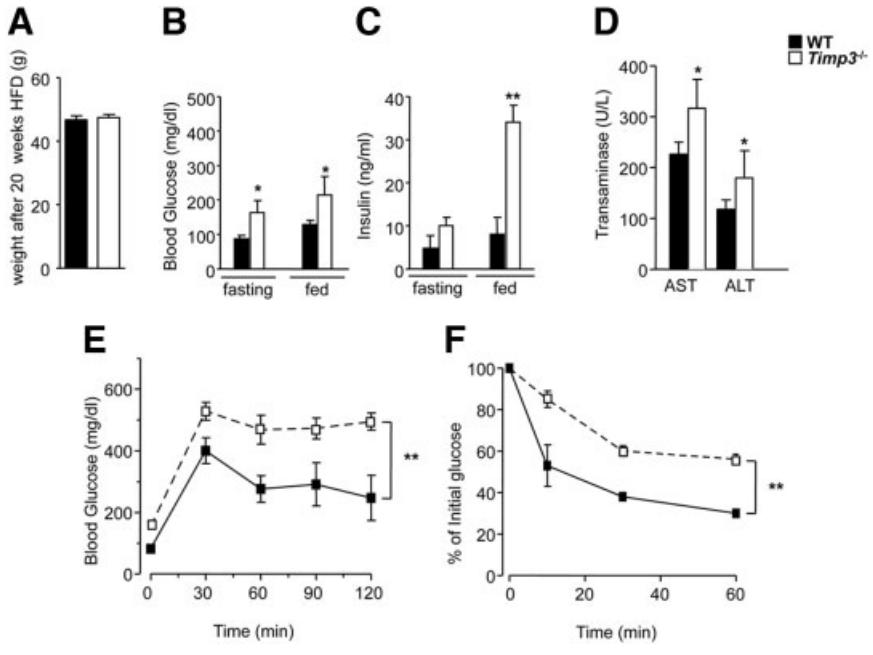

Fig. 3. Impaired glucose tolerance in *Timp3*$^{-/-}$ mice fed a HFD. WT and *Timp3*$^{-/-}$ mice were fed a HFD for 20 weeks and (A) body weight, (B) blood glucose, (C) insulin, and (D) aminotransferase levels were measured. (E-F) WT and *Timp3*$^{-/-}$ mice were fasted overnight and (E) intraperitoneal glucose tolerance test and (F) intraperitoneal insulin tolerance test were performed. Data are expressed as the mean ± SD (n = 6). **$P < 0.005$. *$P < 0.05$.

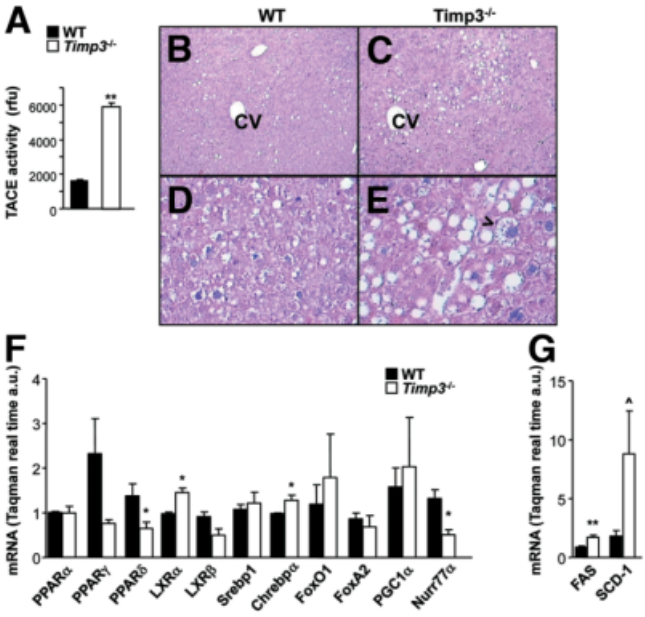

Fig. 4. Steatohepatitis in *Timp3*$^{-/-}$ mice fed a HFD. (A) TACE activity was measured in livers from WT and *Timp3*$^{-/-}$ mice. (B-E) Livers from WT and *Timp3*$^{-/-}$ mice fed a HFD were fixed in formalin, and 5-μm-thick sections were stained with hematoxylin-eosin and Masson's trichrome. Sections were analyzed by way of light microscopy at magnifications of $\times$10 (B,C) and $\times$40 (D,E). (F,G) Expression of transcription factors and enzymes involved in lipid and carbohydrate metabolism was measured using real-time PCR on livers from WT and *Timp3*$^{-/-}$ mice fed a HFD. Data are expressed as the mean $\pm$ SD (n = 3). $^{**}P < 0.005$. $^{*}P < 0.05$. $P = 0.06$.

Nurr77 (Fig. 4F) compared with WT livers. Expression of targets of liver X receptor α and carbohydrate response element binding protein 1 such as fatty acid synthase and stearoyl-coenzyme A desaturase 1 were consequently increased in *Timp3*$^{-/-}$ mice compared with WT controls (Fig. 4G).

Shotgun Proteomics Analysis of Steatohepatitis in Timp3*$^{-/-}$ *and WT Mice Fed a HFD for 20 Weeks. Because our data suggested that TACE activation plays a role in the pathogenesis of nonalcoholic steatohepatitis, we were prompted to use a proteomics-based approach to identify TACE targets linked to controlling lipid and glucose metabolism in the liver. Shotgun proteomics analysis of hepatic lysates from WT and *Timp3*$^{-/-}$ mice revealed 38 differentially expressed proteins in WT versus *Timp3*$^{-/-}$ mice (Table 1). An unbiased systems biology approach showed that Timp3 knockouts carried significantly different signals involving liver fibrosis, damage, steatosis, cholestasis, and hyperbilirubinemia (Supporting Table 1). To seek the best candidates to validate our proteomic approach, we used bioinformatics to identify proteins associated with liver disease and lipid metabolism. Data analysis performed through IPA-Ingenuity software pointed to several proteins in hepatic system disease, amino acid and lipid metabolism, and highlighted adenosine kinase (ADK), methionine adenosyltransferase I/III (MATI/III), glycine *N*-methyltransferase (GNMT), and fatty acid-binding protein 1 (FABP-1) as relevant targets. Supporting Figs. S2 and S3 show representative images of IPA analysis, and proteomic identification data are shown in Supporting Figs. 4 and 5. Interestingly, several of these proteins are involved in the regulation of methionine metabolism.[20,21] Next, liver lysates from WT and *Timp3*$^{-/-}$ mice were immunoblotted to confirm that ADK, MATI/III, and GNMT protein levels were indeed significantly decreased whereas the FABP-1 level was significantly increased in livers of *Timp3*$^{-/-}$ mice compared with WT littermates (Fig. 5A). To control the effect of TACE at the mRNA level, we used quantitative real-time polymerase chain reaction (PCR) to analyze the expression of ADK, methionine adenosysltransferase 1A (MAT1A), GNMT, and fatty acid–binding protein 1 (FABP1) genes and found a pattern comparable with the correspondent protein levels (Fig. 5B). Moreover, we found unchanged expression of methionine adenosysltransferase 2, cystathionine-beta-synthase, and 5,10-methylenetetrahydrofolate reductase—three other enzymes involved in methionine metabolism but not identified by proteomics—suggesting that TACE effects are specific (Supporting Fig. 6A). Analysis of *S*-adenosylmethionine and *S*-adenosylhomocysteine in the liver as well as methionine and homocysteine in the blood confirmed that a HFD has to some extent a different effect on methionine metabolism in *Timp3*$^{-/-}$ mice compared with their WT littermates (Fig. 5C). Because Timp3 controls different families of membrane proteases, we examined whether the proteins identified are linked to TACE activation in synergy with lipotoxicity. Therefore, we adenovirally overexpressed TACE in hepatocytes in the presence or absence of increasing concentrations of palmitic acid. Immunoblot analysis confirmed that ADK, MATI/III, GNMT, and FABP-1 expression was modulated *in vitro* in a manner similar to that observed *in vivo* (Fig. 6A). Analysis of mRNA levels of the same candidates supported that TACE effects are specific (Fig. 6B) due to lack of effect on methionine adenosysltransferase 2, cystathionine-beta-synthase, and 5,10-methylenetetrahydrofolate reductase (Supporting Fig. 6B). Analysis of *S*-adenosylmethionine and *S*-adenosylhomocysteine from cell extracts suggested that the TACE effects on the regulation of methionine metabolism may depend on several conditions, including interaction with lipotoxicity (Supporting Fig. 6C).

Discussion

Epidemiological studies suggest that among the metabolic complications of obesity, NAFLD may evolve into

Table 1. List of Proteins Differentially Expressed in WT and *Timp3*$^{-/-}$ Mice

Accession SwissProt	Description (Symbol)	Score PLGS	WT:Timp3$^{-/-}$ ratio
WT>Timp3$^{-/-}$			
Q91X72	Hemopexin precursor (HPX)	218.67	>5
P97351	40S ribosomal protein S3a (RPS3A)	158.65	>5
P62082	40S ribosomal protein S7 (RPS7)	135.62	>5
P62908	40S ribosomal protein S3 (RPS3)	155.18	>5
P55264	**Adenosine kinase (ADK)**	**193.93**	**>5**
Q61646	Haptoglobin precursor (HPR)	170.37	>5
Q99PG0	Arylacetamide deacetylase (AADAC)	138.27	>5
P48962	ADP/ATP translocase 1 (SLC25A4)	246.33	>5
P68040	Receptor of activated protein kinase C 1 (GNB2L1)	144.83	>5
Q91VS7	Microsomal glutathione S-transferase 1 (MGST1)	142.31	>5
Q99LB7	Sarcosine dehydrogenase, mitochondrial precursor (SARD)	326.9	>5
P19157	Glutathione S-transferase P 1 (GSTP1)	350.31	2.03
Q9QXF8	**Glycine N-methyltransferase (GNMT)**	**299.32**	**1.73**
Q8R0Y6	10-formyltetrahydrofolate dehydrogenase (ALDH1L1)	562.33	1.67
P11725	Ornithine carbamoyltransferase, mitochondrial precursor (OTC)	304.39	1.55
P16460	Argininosuccinate synthase (Citrulline–aspartate ligase) (ASS1)	904.66	1.51
Q61176	Arginase-1 (Liver-type arginase) (ARG1)	582.61	1.51
P15105	Glutamine synthetase (GLUL)	259.51	1.48
P20029	78 kDa glucose-regulated protein precursor (HSPA5)	426.35	1.46
Q8C196	Carbamoyl-phosphate synthase (CPS1)	2003.64	1.43
Q63836	Selenium-binding protein 2 (SELENBP1)	337.87	1.42
P35505	Fumarylacetoacetase (FAH)	291.02	1.4
P62806	Histone H4	283.78	1.39
P50247	Adenosylhomocysteinase (AHCY)	334.52	1.38
P06151	L-lactate dehydrogenase A chain (LDHA)	343.91	1.38
Q91X83	**Methionine adenosyltransferase 1 (MATI/III)**	**362.33**	**1.38**
P17156	Heat shock-related 70 kDa protein 2 (Heat shock protein 70.2) (HSPA2)	284.56	1.34
Q63880	Liver carboxylesterase 31 precursor (Esterase- 31) (CES3)	325.06	1.34
P49429	4-hydroxyphenylpyruvate dioxygenase (HPD)	325.2	1.34
P47738	Aldehyde dehydrogenase, mitochondrial precursor (ALDH2)	599.59	1.31
P27773	Protein disulfide-isomerase A3 precursor (PDIA3)	218.04	1.31
WT<Timp3$^{-/-}$			
Q64442	Sorbitol dehydrogenase (SORD)	348.14	<0.2
P48036	Annexin A5 (ANXA5)	132.75	<0.2
P56395	Cytochrome b5 (CYB5A)	156.26	<0.2
P56391	Cytochrome c oxidase subunit VIb isoform 1 (COX6B1)	88.26	<0.2
Q01853	Transitional endoplasmic reticulum ATPase (VCP)	267.36	<0.2
P12710	**Fatty acid-binding protein, liver (FABP1)**	**330.68**	**0.64**
P16015	Carbonic anhydrase 3 (CA3)	570.14	0.53

Boldface type indicates proteins confirmed by way of western blotting in tissues from WT and *Timp3*$^{-/-}$ mice and in hepatocytes infected with adenovirus encoding TACE.

steatohepatitis, cirrhosis, or hepatocellular carcinoma.[1] Experimental models have suggested that direct lipotoxicity (increased circulating free fatty acid) and glucotoxicity (aggravating insulin resistance) may interfere with regulation of lipid and carbohydrate metabolism in the liver, resulting in steatosis and consequently progressive liver damage.[2,3] Although several mediators accompanying the progression from simple steatosis to steatohepatitis and to more severe degenerative diseases have been identified, the mechanisms explaining how metabolic toxicity initiates the inflammatory burden are still incompletely characterized. We recently reported that the TACE/Timp3 dyad, which regulates the bioavailability of cytokines and growth factors such as TNF-α and epidermal growth factor receptor ligands, functions to amplify the metabolic damage induced by genetic or environmental insulin resistance.[10-12]

Recent functional genomic and proteomic analysis performed toward dissecting pathways in hepatic steatosis pathogenesis have revealed several ADAM enzymes that are well expressed in the liver, although their functional role has been inadequately studied.[22-24] TACE is the prototypical alpha secretase, identified as the major enzyme involved in shedding TNF-α. This cytokine is believed to play a role in the progression of NAFLD due to its ability to increase inflammatory signals by way of nuclear factor κB activation and affect insulin action via activation of JNK/IKKβ kinases. Our data revealed a role for liver-specific TACE activity in the onset of hepatic steatosis and consequent tissue degeneration and showed that liver is

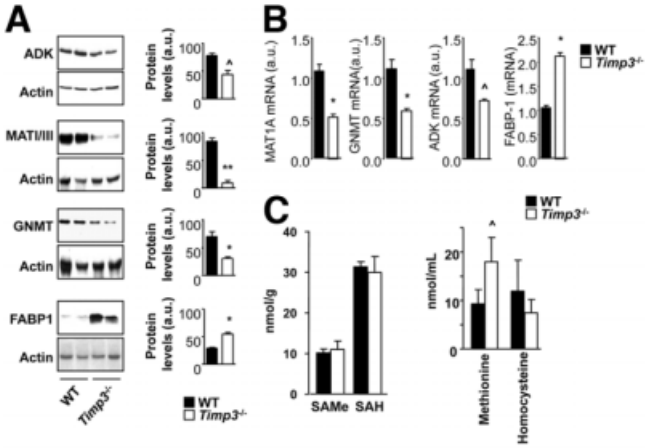

Fig. 5. TACE modulates expression of key elements involved in hepatic steatosis. Livers from WT and *Timp3* $^{-/-}$ mice fed a HFD were analyzed by way of (A) western blotting and (B) real-time PCR. Data are expressed as the mean ± SD (n = 3). $^{**}P < 0.005$. $^{*}P < 0.05$. $P = 0.06$. (C) *S*-adenosylmethionine, *S*-adenosylhomocysteine levels in liver extracts and methionine/homocysteine levels in blood from from WT and *Timp3*$^{-/-}$ mice fed a HFD (n = 4 per group). $P = 0.06$.

the first tissue to exhibit increased TACE activity upon metabolic stress. TACE activation is consequent to concomitant actions of intracellular signals mediated by protein kinase C and extracellular signal-regulated kinase as well as reduction of its endogenous inhibitor Timp3. Our data suggest that both fatty acids and stress-activated kinases such as JNK may also play a role in TACE activation. We further demonstrate that TACE reduces the ability of insulin to regulate the AKT/FoxO1/GSK3 pathway, the major controller of gluconeogenesis and lipogenesis.[25,26] Although increased release of TNF-α may explain TACE effects on insulin signaling and hepatic steatosis, we cannot exclude that other surface proteins shed by TACE may have a part in this process.

To study the *in vivo* effects of TACE activation, we used the *Timp3* knockout model that is characterized by increased TACE activity in the liver. Because it appears that metabolic toxicity induces the activation of this enzyme, we subjected *Timp3*$^{-/-}$ mice to prolonged metabolic stress. Our data suggest that prolonged unrestrained TACE activity contributes to liver degeneration following lipid overload. Histological analysis revealed that *Timp3*$^{-/-}$ mice manifest macrovesicular steatosis and lobular degeneration compared with their WT littermates. This phenotype may be explained at least in part by increased expression of transcription factors involved in lipogenesis such as liver X receptor α and carbohydrate response element binding protein, supported by the increased expression of their substrates fatty acid synthase and stearoyl CoA desaturase 1.[2]

Because TACE regulates several factors potentially affecting inflammation, metabolic homeostasis, fibrosis, and cell cycle, we used a shotgun proteomic approach to identify proteins linked to the steatosis phenotype in *Timp3*$^{-/-}$ mice that could be targets of TACE. Recent studies have shown that a proteomic approach linked to bioinformatic analysis is a useful tool to identify novel targets in the pathogenesis of NAFLD. Our analysis clearly identified liver diseases as the most representative for the submitted data, supporting the validity of our observations. Moreover, this unbiased analysis also indicated liver fibrosis and steatosis as the top associated disease processes that differentiate *Timp3*$^{-/-}$ from WT mice. Our results led to identify several proteins potentially important for the phenotype showed by *Timp3*$^{-/-}$ mice fed a HFD. To substantiate our proteomics findings, we elected to measure those proteins linked to steatosis through both a bioinformatic approach and evidence from the literature. Although we cannot rule out the contribution of the other identified proteins—especially those with the highest deviation—we observed that a cluster of down-regulated proteins was linked to methionine metabolism, a pathway known to affect steatosis in mouse models.[20,21] Among the proteins most significantly decreased in *Timp3*$^{-/-}$ mice was ADK, which was implicated in protection against hepatic steatosis through the regulation of adenosine levels.[27] Both *MAT1A* and *GNMT* knockouts also support our findings.[28,29] In fact, deficiency of MATI/III enzyme is characterized by macrovesicular steatosis and increased expression of proliferative signals with decreased *S*-adenosylmethionine and increased methionine.[28] By contrast, GNMT deficiency leads to steatosis and hepatocellular carcinoma in mice characterized by increased *S*-adenosylmethionine but increased methionine.[29] The definition of the role of Timp3

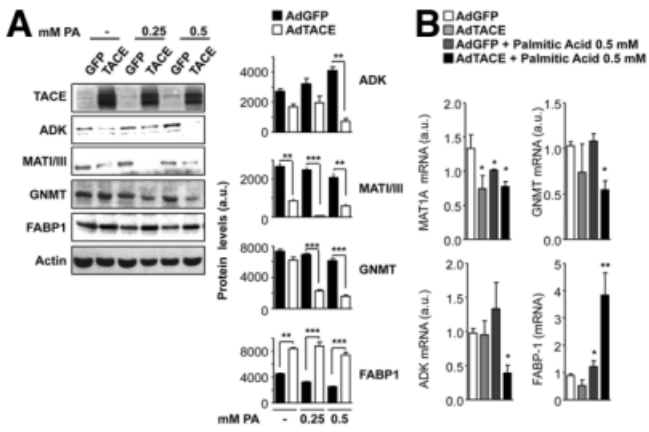

Fig. 6. TACE effects on key elements of methionine metabolism in hepatocyes in culture. SV40-transformed hepatocytes were infected with adeno-GFP or adeno-GFP-TACE and then treated overnight with different concentrations of palmitic acid. Protein and mRNA levels were analyzed by way of (A) western blotting and (B) real-time PCR (n = 3). $^{*}P < 0.05$. $^{**}P < 0.01$. $^{***}P < 0.001$.

and TACE in the regulation of methionine metabolism will require further studies, although the observation of increased methionine levels in *Timp3*$^{-/-}$ mice is a common feature of both *MAT1A* and *GNMT* and suggests that these genes play a role in the phenotype described here.[21]

Among up-regulated signals we found FABP1; mice deficient in FABP1 are protected from liver steatosis induced by a HFD, consistent with the hypothesis that increased FABP1 expression, as found in *Timp3*$^{-/-}$ mice and in hepatocytes over expressing TACE, may contribute to an opposite phenotype.[30]

In conclusion, our data support the concept that TACE is a novel regulator of hepatic metabolism that is activated in the course of metabolic toxicity induced by an HFD and contributes to the development of NAFLD through multiple mechanisms.

References

1. Vuppalanchi R, Chalasani N. Nonalcoholic fatty liver disease and nonalcoholic steatohepatitis: selected practical issues in their evaluation and management. HEPATOLOGY 2009;49:306-317.
2. Postic C, Girard J. The role of the lipogenic pathway in the development of hepatic steatosis. Diabetes Metab 2008;34:643-648.
3. Postic C, Girard J. Contribution of de novo fatty acid synthesis to hepatic steatosis and insulin resistance: lessons from genetically engineered mice. J Clin Invest 2008;118:829-838.
4. Adachi M, Osawa Y, Uchinami H, Kitamura T, Accili D, Brenner DA. The forkhead transcription factor FoxO1 regulates proliferation and transdifferentiation of hepatic stellate cells. Gastroenterology 2007;132:1434-1446.
5. Feldstein AE, Werneburg NW, Canbay A, Guicciardi ME, Bronk SF, Rydzewski R, et al. Free fatty acids promote hepatic lipotoxicity by stimulating TNF-alpha expression via a lysosomal pathway. HEPATOLOGY 2004;40:185-194.
6. Murphy G, Murthy A, Khokha R. Clipping, shedding and RIPping keep immunity on cue. Trends Immunol 2008;29:75-82.
7. Reddy AB, Ramana KV, Srivastava S, Bhatnagar A, Srivastava SK. Aldose reductase regulates high glucose-induced ectodomain shedding of tumor necrosis factor (TNF)-alpha via protein kinase C-delta and TNF-alpha converting enzyme in vascular smooth muscle cells. Endocrinology 2009; 150:63-74.
8. Soond SM, Everson B, Riches DW, Murphy G. ERK-mediated phosphorylation of Thr735 in TNFalpha-converting enzyme and its potential role in TACE protein trafficking. J Cell Sci 2005;118:2371-2380.
9. Chen CD, Podvin S, Gillespie E, Leeman SE, Abraham CR. Insulin stimulates the cleavage and release of the extracellular domain of Klotho by ADAM10 and TACE. Proc Natl Acad Sci U S A 2007;104:19796-19801.
10. Federici M, Hribal ML, Menghini R, Kanno H, Marchetti V, Porzio O, et al. Timp3 deficiency in insulin receptor-haploinsufficient mice promotes diabetes and vascular inflammation via increased TNF-alpha. J Clin Invest 2005;115:3494-3505.
11. Serino M, Menghini R, Fiorentino L, Amoruso R, Mauriello A, Lauro D, et al. Mice heterozygous for tumor necrosis factor-alpha converting enzyme are protected from obesity-induced insulin resistance and diabetes. Diabetes 2007;56:2541-2546.
12. Menghini R, Menini S, Amoruso R, Fiorentino L, Casagrande V, Marzano V, et al. Tissue inhibitor of metalloproteinase 3 deficiency causes hepatic steatosis and adipose tissue inflammation in mice. Gastroenterology 2009; 136:663-672.
13. Menghini R, Marchetti V, Cardellini M, Hribal ML, Mauriello A, Lauro D, et al. Phosphorylation of GATA2 by Akt increases adipose tissue differentiation and reduces adipose tissue-related inflammation: a novel pathway linking obesity to atherosclerosis. Circulation 2005;111:1946-1953.
14. Hribal ML, Nakae J, Kitamura T, Shutter JR, Accili D. Regulation of insulin-like growth factor-dependent myoblast differentiation by Foxo forkhead transcription factors. J Cell Biol 2003;162:535-541.
15. Kim JJ, Park BC, Kido Y, Accili D. Mitogenic and metabolic effects of type I IGF receptor overexpression in insulin receptor-deficient hepatocytes. Endocrinology 2001;142:3354-3360.
16. Mohammed FF, Smookler DS, Taylor SE, Fingleton B, Kassiri Z, Sanchez OH, et al. Abnormal TNF activity in Timp3-/- mice leads to chronic hepatic inflammation and failure of liver regeneration. Nat Genet 2004; 36:969-977.
17. Vissers JP, Langridge JI, Aerts JM. Analysis and quantification of diagnostic serum markers and protein signatures for Gaucher disease. Mol Cell Proteomics 2007;6:755-766.
18. Ronci M, Bonanno E, Colantoni A, Pieroni L, Di Ilio C, Spagnoli LG, et al. Protein unlocking procedures of formalin-fixed paraffin-embedded tissues: application to MALDI-TOF imaging MS investigations. Proteomics 2008;8:3702-3714.
19. Wang W, Kramer PM, Yang S, Pereira MA, Tao L. Reversed-phase high-performance liquid chromatography procedure for the simultaneous determination of *S*-adenosyl-L-methionine and *S*-adenosyl-L-homocysteine in mouse liver and the effect of methionine on their concentrations. J Chromatogr B Biomed Sci Appl 2001;762:59-65.
20. Kotb M, Mudd SH, Mato JM, Geller AM, Kredich NM, Chou JY, et al. Consensus nomenclature for the mammalian methionine adenosyltransferase genes and gene products. Trends Genet 1997;13:51-52.
21. Mato JM, Martínez-Chantar ML, Lu SC. Methionine metabolism and liver disease. Annu Rev Nutr 2008;28:273-293.
22. Calvert VS, Collantes R, Elariny H, Afendy A, Baranova A, Mendoza M, et al. A systems biology approach to the pathogenesis of obesity-related nonalcoholic fatty liver disease using reverse phase protein microarrays for multiplexed cell signaling analysis. HEPATOLOGY 2007;46:166-172.
23. Diamond DL, Proll SC, Jacobs JM, Chan EY, Camp DG 2nd, Smith RD, et al. HepatoProteomics: applying proteomic technologies to the study of liver function and disease. HEPATOLOGY 2006;44:299-308.
24. Younossi ZM, Baranova A, Ziegler K, Del Giacco L, Schlauch K, Born TL, et al. A genomic and proteomic study of the spectrum of nonalcoholic fatty liver disease. HEPATOLOGY 2005;42:665-674.
25. Matsumoto M, Pocai A, Rossetti L, Depinho RA, Accili D. Impaired regulation of hepatic glucose production in mice lacking the forkhead transcription factor Foxo1 in liver. Cell Metab 2007;6:208-216.
26. Matsumoto M, Han S, Kitamura T, Accili D. Dual role of transcription factor FoxO1 in controlling hepatic insulin sensitivity and lipid metabolism. J Clin Invest 2006;116:2464-2472.
27. Boison D, Scheurer L, Zumsteg V, Rülicke T, Litynski P, Fowler B, et al. Neonatal hepatic steatosis by disruption of the adenosine kinase gene. Proc Natl Acad Sci U S A 2002;99:6985-6990.
28. Lu SC, Alvarez L, Huang ZZ, Chen L, An W, Corrales FJ, et al. Methionine adenosyltransferase 1A knockout mice are predisposed to liver injury and exhibit increased expression of genes involved in proliferation. Proc Natl Acad Sci U S A 2001;98:5560-5565.
29. Martínez-Chantar ML, Vázquez-Chantada M, Ariz U, Martínez N, Varela M, Luka Z, et al. Loss of the glycine N-methyltransferase gene leads to steatosis and hepatocellular carcinoma in mice. HEPATOLOGY 2008;47: 1191-1199.
30. Newberry EP, Xie Y, Kennedy SM, Luo J, Davidson NO. Protection against Western diet-induced obesity and hepatic steatosis in liver fatty acid-binding protein knockout mice. HEPATOLOGY 2006;44:1191-1205.